PHYSICAL REVIEW B **84**, 024422 (2011)

Magnetoelectric coupling at the interface of $BiFeO_3/La_{0.7}Sr_{0.3}MnO_3$ multilayers

M. J. Calderón,[1] S. Liang,[2,3] R. Yu,[4] J. Salafranca,[5] S. Dong,[6] S. Yunoki,[7,8] L. Brey,[1] A. Moreo,[2,3] and E. Dagotto[2,3]
[1]*Instituto de Ciencia de Materiales de Madrid ICMM-CSIC, Cantoblanco, 28049 Madrid, Spain*
[2]*Department of Physics and Astronomy, University of Tennessee, Knoxville, Tennessee 37996, USA*
[3]*Materials Science and Technology Division, Oak Ridge National Lab, Oak Ridge, Tennessee 37831, USA*
[4]*Department of Physics and Astronomy, Rice University, Houston, Texas 77005, USA*
[5]*Departamento de Física Aplicada III, Universidad Complutense de Madrid, 28040 Madrid, Spain*
[6]*Department of Physics, Southeast University, Nanjing 211189, China*
[7]*Computational Condensed Matter Physics Laboratory, RIKEN, Wako, Saitama 351-0198, Japan*
[8]*CREST, Japan Science and Technology Agency (JST), Kawaguchi, Saitama 332-0012, Japan*
(Received 21 January 2011; revised manuscript received 8 March 2011; published 15 July 2011)

Electric-field controlled exchange bias in a heterostructure composed of the ferromagnetic manganite $La_{0.7}Sr_{0.3}MO_3$ and the ferroelectric antiferromagnetic $BiFeO_3$ has recently been demonstrated experimentally. By means of a model Hamiltonian, we provide a possible explanation for the origin of this magnetoelectric coupling. We find, in agreement with experimental results, a net ferromagnetic moment at the $BiFeO_3$ interface. The induced ferromagnetic moment is the result of the competition between the e_g-electron double exchange and the t_{2g}-spin antiferromagnetic superexchange that dominates in bulk $BiFeO_3$. The balance of these simultaneous ferromagnetic and antiferromagnetic tendencies is strongly affected by the interfacial electronic charge density, which, in turn, can be controlled by the $BiFeO_3$ ferroelectric polarization.

DOI: 10.1103/PhysRevB.84.024422 PACS number(s): 75.47.Gk, 75.10.−b, 75.30.Kz, 75.50.Ee

I. INTRODUCTION

The quest for efficient electric-field control of magnetic properties has encouraged research on materials with a strong coupling between the magnetic and electric degrees of freedom.[1] Such a control would find applications in magnetic-field storage and sensors, constituting a major step forward in the field of spintronics. However, so far no bulk material seems to possess the required characteristics, including working near room temperature. For these reasons, the field-effect device presented in Ref. 2 signals a new route[3] to achieving those goals by growing a few-nanometers-thick layer of $La_{0.7}Sr_{0.3}MnO_3$ (LSMO), a ferromagnetic (FM) metal, on an antiferromagnetic (AFM) and ferroelectric (FE) material, $BiFeO_3$ (BFO).[2,4] These experiments provided evidence for an induced FM moment in BFO at the interface. This magnetic moment is strongly affected by the BFO polarization, which results in an electric-field control of the LSMO exchange bias (EB), and concomitant control of the LSMO magnetization.

Magnetic moments induced at the interface of perovskite-based oxide materials have been previously reported. For example, a net magnetic moment was induced in an AFM manganite when grown in a multilayer with a FM manganite,[5,6] at the interface of a superconducting cuprate with $La_{0.67}Ca_{0.33}MO_3$,[7] and at LSMO/$SrTiO_3$ interfaces.[8] Electronic energy loss measurements indicate that a charge redistribution takes place.[7,8] Theoretically, the origin of the induced magnetic moment in Ref. 5 was explained in terms of charge transfer and a double exchange (DE) type interaction.[9] Charge transfer, together with orbital reconstruction, is also believed to play a role at cuprate/$La_{0.67}Ca_{0.33}MO_3$ interfaces.[7] In Refs. 4 and 10, the BFO-induced FM moment in LSMO/BFO heterostructures was attributed to Fe-Mn hybridization, which is associated with charge transfer. The recently observed coupling of the EB with an induced magnetization near the interface, simultaneously controlled by the FE polarization,[2,4] defines a new complex phenomenon that requires a better theoretical understanding.[11]

In this paper, a microscopic model for the transition-metal d electrons is shown to explain the main properties of the BFO/LSMO interface. Within this model, the magnetic moments of the Fe ions develop a net FM moment close to the interface as a consequence of both charge and orbital redistribution, while they remain AFM ordered far from the interface. Interestingly, the direction and magnitude of the BFO moment with respect to the magnetization of the LSMO layer depend on the charge density at the interface. Small changes in the charge density due to the switching of the FE polarization in BFO produces large modifications in the direction of the magnetic moment induced in the Fe ions. This leads to the experimentally observed EB.[2] Our scenario is qualitatively different from that proposed in Ref. 4, which is based on the first LSMO layer, and that of Ref. 11, which requires a spin-orbit coupling.

In Sec. II, we introduce the microscopic model for the d electrons of both BFO and LSMO. In Sec. III, the magnetic reconstruction that takes place at the BFO/LSMO interface as well as the modifications induced by the BFO ferroelectricity are described. We end in Sec. IV with a discussion of our results in light of the reported experiments and the conclusions.

II. MODEL

Figure 1 sketches the $4 \times 4 \times 12$ supercell used in our calculations. Bulk LSMO (BFO) is in a FM (G-type AFM) state. A possible magnetic reconstruction near the interface is also indicated. Departures from the cubic perovskite lattice, as induced by strain and ferroelastic effects, are ignored for simplicity. The z-axis size (eight layers for LSMO and four for BFO) is selected such that bulk behavior is recovered at the center of the composing films.

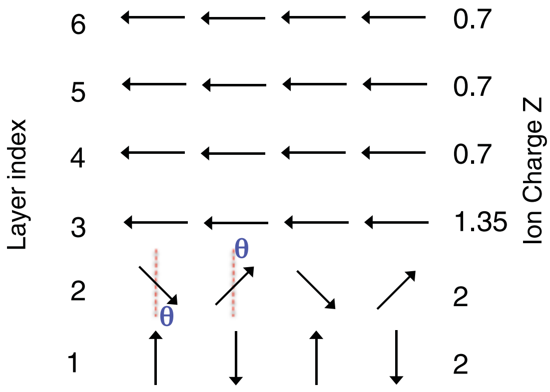

FIG. 1. (Color online) Proposed spin order in the BFO-LSMO heterostructure (only half of the structure is shown, the other half is symmetric). The two first (1,2) and two last (11,12) planes have ionic charge $Z = +2$, and correspond to BFO. Layers 3 and 10 define the interface, with $Z = (0.7 + 2)/2$. The central planes (4 to 9) have $Z = 0.7$ and correspond to LSMO.

Magnetism in the heterostructure arises from the transition-metal d electrons. In manganites, the three t_{2g} electrons are localized and are approximated by a single classical spin. AFM superexchange with neighboring sites is introduced via a Heisenberg interaction.[12] The quantum itinerant e_g electrons are described by the DE model in the infinite Hund's coupling limit. Several aspects of the rich physics of bulk[12–15] and heterostructured manganites[9,16–18] have been successfully addressed within this approach. However, model Hamiltonian approaches have not been used before for BFO. Here we use a microscopic model for BFO to describe the itinerant electrons and the magnetism while the ferroelectricity will be included at the phenomenological level.

To properly consider the effects of charge leakage and orbital hybridization at the interface,[10] the e_g electrons of *both* BFO and LSMO must be treated on an equal footing. The model is

$$H = -\sum_{\langle i,j\rangle,\alpha,\beta} t_{ij} O^{\alpha\beta}_{i-j} \Omega_{ij} c^{\dagger}_{i\alpha} c_{j\beta} + \sum_{\langle i,j\rangle} J^{\mathrm{AFM}}_{ij} \mathbf{S}_i \cdot \mathbf{S}_j + \sum_i (\tilde{\phi}_i + V_i - \mu) n_i. \qquad (1)$$

Here, $\mathbf{S}_i$ represents the t_{2g} spin at site i, located either at the LSMO or the BFO side of the heterostructure, while J^{AFM}_{ij} is the AFM superexchange parameter. $c^{\dagger}_{i\alpha}$ creates an electron on an orbital centered at the transition-metal site with e_g symmetry: $\alpha, \beta = |3z^2 - r^2\rangle, |x^2 - y^2\rangle$. The hopping term is modulated by the DE factor Ω_{ij},[12] which depends on the angle between $\mathbf{S}_i$ and $\mathbf{S}_j$ such that it is maximum for parallel alignment of spins at neighboring sites and zero for antiparallel alignment. Hopping also depends on the overlap between the α and β orbitals along the direction i-j through the geometric factor $O^{\alpha\beta}_{i-j}$.[12] In principle, the hopping parameters t_{ij} should depend on the material, and would be affected by lattice distortions near the interface. We simplify the calculation by assuming a uniform hopping parameter for the whole heterostructure ($t_{ij} = t$) (t is the energy unit). The superexchange coupling is more sensitive to changes in lattice constants, hence each material will be characterized by a different J_{AFM}.

In general, the DE term in Eq. (1) favors FM configurations that optimize the kinetic energy, while the superexchange term favors AFM phases. The third term contains the different contributions to the site potential. Long-range Coulomb interactions are essential to control charge transfer across the interface. This is included in the Hartree approximation by setting

$$\tilde{\phi}_i = \alpha \sum_{j \neq i} \frac{n_j - Z_j}{|\vec{r}_i - \vec{r}_j|}. \qquad (2)$$

The Coulomb interaction strength is regulated by the parameter α, here assumed equal to $2t$.[9,19] For each x-y plane, Z as illustrated in Fig. 1 is considered, and the approximation is made that the background consists of point charges that occupy the transition-metal sites. $Z = 2$ for BFO, while $Z = 0.7$ for LSMO. An interfacial layer is considered with an intermediate value of Z to account for possible diffusions and different chemical environments of the transition-metal ions at the interface. V_i includes the effect of the band offset between BFO and LSMO V_{offset}, and the surface charge density due to ferroelectricity V_0. The band offset is difficult to estimate, though it is expected to be small. From BFO electronic affinity[20] and LSMO work functions,[21] we estimate $V_{\mathrm{offset}} = V_{\mathrm{LSMO}} - V_{\mathrm{BFO}} \sim 0.6t$. However, V_{offset} is treated here as an adjustable parameter: it is first set to zero and the results are then checked against moderate changes in its value. The chemical potential μ is chosen so that the overall system remains charge-neutral.

Several approximations are implicit in Eq. (1). While the intraorbital Hubbard interaction U is effectively infinite due to the infinite Hund's coupling implicit in DE, the interorbital U' might be important. However, it has been checked that introducing a moderate $U' = 2t$ at the mean-field level does not significantly affect the results. The coupling to Jahn-Teller lattice modes is not included either, but it is widely accepted that they do not play an important role in LSMO or BFO at any of the interfacial fillings of the d bands. For each set of parameters and different t_{2g} spin configurations, Eq. (1) was solved by exact diagonalization. Periodic boundary conditions are used, with a $5 \times 5 \times 1$ mesh in reciprocal space.

Another approximation contained in our model Hamiltonian is the focus on the Mn ions and the direct transfer of charge from one to the other via the electronic hopping terms, as opposed to having explicitly the oxygen degree of freedom as an intermediate step and allowing for the O-Mn hopping of the mobile electrons.[22] This approximation, considered since the early developments in manganites in the 1950s, has successfully described the rich phase diagram of manganites in the bulk,[12] and recent investigations have shown that even the colossal magnetoresistance (CMR) effect is reproduced qualitatively by this procedure.[14] Thus, for our present effort, which is among the first to address the BFO/LSMO interface via model studies, the use of the same starting model as in the bulk is reasonable. However, the possible relevance of oxygens for a proper description of manganites has been emphasized in some investigations,[23] and only future work can establish whether successful bulk approaches can be extended to the study of interfaces. In our results below, the oxygens will be neglected.

III. RESULTS

Our first important result is sketched in Fig. 1. While LSMO remains FM, and most of BFO remains in the G-AFM state, a magnetic reconstruction takes place in the last atomic layer of BFO. The perpendicular orientation of the spins in bulk BFO (layer 1) relative to LSMO gives lower energy than a parallel orientation. The magnetic state in the last BFO layer can be characterized by a single angle θ, defined in Fig. 1, which determines the magnetization of BFO close to the interface, M_{BFO}. For $\theta = \pi/2$, the last layer of BFO is FM but antiparallel to the LSMO magnetization, thus $M_{\mathrm{BFO}} = -1$; for $\theta = 3\pi/2$, the last layer of BFO is FM and parallel to the LSMO magnetization, $M_{\mathrm{BFO}} = 1$; and for $\theta = 0,2\pi$, there is no net magnetization in BFO. Regardless of the ground-state value of θ, the main magnetic reconstruction is confined to the BFO outermost layer, since spin canting at the LSMO interfacial atomic layer is small. These results are remarkably independent of details, such as whether there is an interfacial layer with intermediate background charge. It also holds for several values of J_{AFM}, as long as they are reasonable (for the proper bulk phase diagram: $J_{\mathrm{AFM}}^{\mathrm{LSMO}} < 0.1; 0.1 < J_{\mathrm{AFM}}^{\mathrm{BFO}} < 0.2$). $J_{\mathrm{AFM}}^{\mathrm{interface}}$ (between layers 2 and 3) is expected to be some average of $J_{\mathrm{AFM}}^{\mathrm{LSMO}}$ and $J_{\mathrm{AFM}}^{\mathrm{BFO}}$. For simplicity, we use $J_{\mathrm{AFM}} = J_{\mathrm{AFM}}^{\mathrm{interface}} = J_{\mathrm{AFM}}^{\mathrm{BFO}}$ and $J_{\mathrm{AFM}}^{\mathrm{LSMO}} = 0$.

Figure 2 illustrates the energy as a function of θ for different values of J_{AFM}. At small J_{AFM}, the energy is minimized at $\theta = 3\pi/2$: the BFO interfacial layer is FM and parallel to the metallic LSMO and DE dominates. As J_{AFM} increases, the minimum near $3\pi/2$ moves toward 2π. In addition, the minimum near $\pi/2$ decreases in energy and eventually has the lowest energy. In this case, the last layer of BFO is FM and antiparallel to the LSMO magnetization. These trends are summarized in the inset of Fig. 2, where the magnetization induced in the last layer of BFO is plotted as a function of J_{AFM}. The magnetization rotation (from $\theta = 3\pi/2$ to $\pi/2$) occurs at $J_{\mathrm{AFM}} \sim 0.12t$ and there is some small canting for $0.07t \lesssim J_{\mathrm{AFM}} \lesssim 0.11t$. For $J_{\mathrm{AFM}} \gtrsim 0.16t$, the AFM coupling is stronger than the DE and the canting angle is zero, namely, the interfacial BFO layer is AFM as in bulk. Several results obtained in the simplified discussion presented here, such as Fig. 2 and others based on the simple assumption that the interfacial behavior is characterized by a single angle θ, were also confirmed numerically using $4 \times 4 \times 8$ clusters, the Poisson equation, and a minimization algorithm for the t_{2g} classical spins.[24]

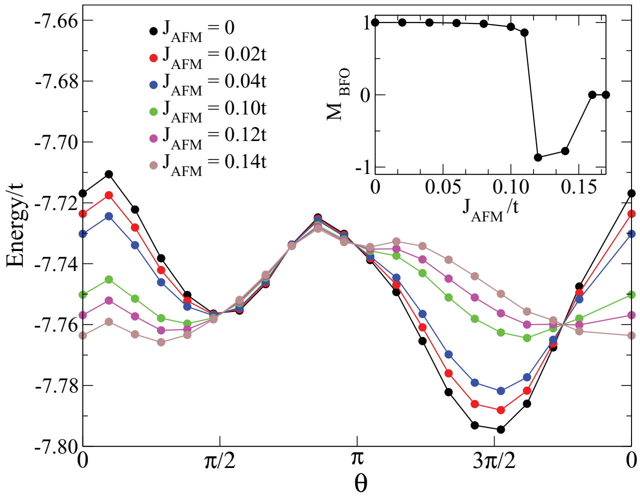

FIG. 2. (Color online) Main panel: Energy vs canting angle θ for different values of J_{AFM}. Inset: Value of the magnetization induced at the interfacial plane of BFO vs J_{AFM}, as given by the position of the minima in the main panel.

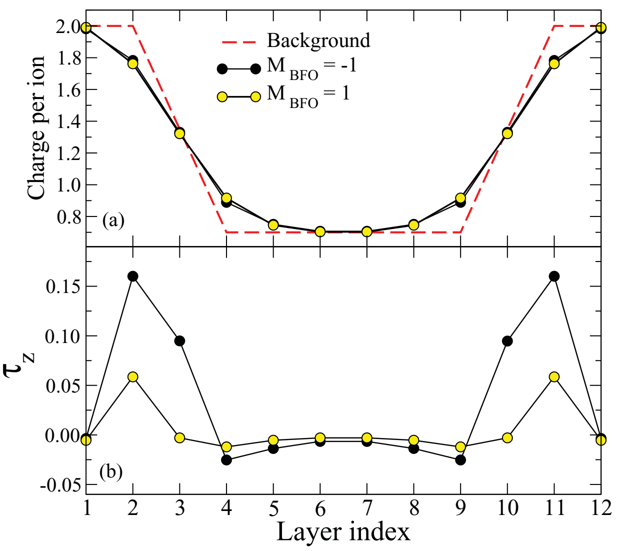

FIG. 3. (Color online) (a) Electronic charge for canting angles $\theta \sim \pi/2$ and $\theta \sim 3\pi/2$ (the dashed line is the positive charge background). The charge-density distribution depends only slightly on θ. (b) Orbital order described by the expectation value of $\langle \tau_z \rangle = n_{x^2-y^2} - n_{3z^2-r^2}$. The e_g orbitals are equally populated ($\langle \tau_z \rangle = 0$) at the BFO and LSMO bulk layers.

The observed charge redistribution and orbital reconstruction confirm the importance of the DE mechanism. Figure 3 shows the charge n_i and orbital polarization $\langle \tau_z \rangle = n_{x^2-y^2} - n_{3z^2-r^2}$ for two values of θ. The e_g-charge profile is mainly determined by the background charge except at the interface planes, where there is a charge redistribution whose extension is controlled by the parameter α:[16] holes at the last atomic plane of BFO and extra electrons at LSMO favor a kinetic-energy gain. For $M_{\mathrm{BFO}} = -1$, the hopping between LSMO and the interfacial BFO layer is suppressed. However, even in this case the Fe d orbitals are not completely filled, and some kinetic-energy gain occurs, mainly within the x-y plane. This asymmetry is evidenced by a nonzero orbital polarization $\langle \tau_z \rangle$, at both sides of the interface (layers 2, 3, 10, and 11). Since there is no electron-lattice coupling here, the orbital polarization necessarily arises from asymmetries in the orbital filling due to kinetic-energy gain. For $M_{\mathrm{BFO}} = 1$, there is hopping across the interface and a significant orbital polarization appears only at the BFO side (layers 2 and 11). The positive orbital polarization is caused by the suppression of the hopping in the z direction due to the filled bands of bulk BFO leading to an enhancement of the hopping in the x-y

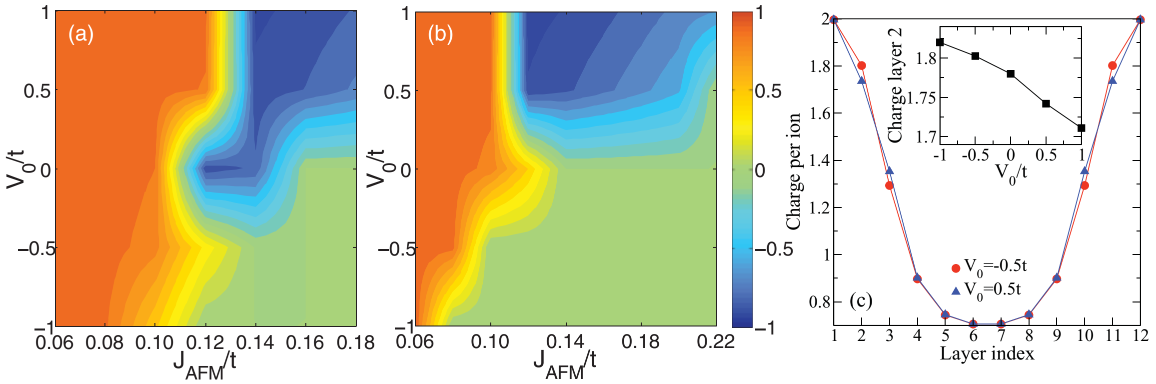

FIG. 4. (Color online) Magnetization induced in BFO (M_{BFO}) as a function of J_{AFM} and V_0 for (a) $V_{\mathrm{offset}} = 0$ and (b) $V_{\mathrm{offset}} = 0.6t$. (c) Electronic charge in the heterostructure for $V_0 = -0.5t$ and $V_0 = 0.5t$. Inset: charge at layer 2 for $-1t \leqslant V_0 \leqslant 1t$.

plane. A larger kinetic energy in this case compensates for the Coulomb energy cost of an e_g density that further deviates from the background value. Although the difference in charge profile for the two angles is small, it plays an important role in the phenomena discussed next.

Consider now the effect of the BFO FE polarization. In our study, we assume that the main effect of switching the FE polarization is to modify the induced charge density at the FE surface. As a consequence, the FE nature of BFO makes the heterostructure work as a field-effect device.[2] The direction of the FE polarization is modeled by introducing an additional potential V_0 at the surface of BFO (layers 2 and 11) which attracts ($V_0 < 0$) or repels ($V_0 > 0$) the charge [see Fig. 4(c)]. Figure 4, our main result, shows the value of the induced magnetization in BFO, M_{BFO}, as a function of J_{AFM} and V_0, for (a) zero band offset, and (b) $V_{\mathrm{offset}} = 0.6t$. For small values of J_{AFM}, a FM BFO layer appears at the interface, parallel to the magnetization on LSMO ($\theta = 3\pi/2$). For larger values of J_{AFM} and an attractive V_0, the AFM solution ($\theta = 0$) is obtained. This is due to the fact that increasing the density of charge toward 2 produces a decrease in kinetic energy, so the gain in superexchange energy dominates. For large values of J_{AFM} and repulsive V_0, a FM BFO layer is obtained that is antiparallel to the magnetization on LSMO ($\theta = \pi/2$). This is due to the decrease of the charge density (away from 2) at the interface, which produces an increase of the x-y plane kinetic energy, while the superexchange term gains energy by making the spins of layers 2 and 3 antiparallel. Equivalent results are found for different values of the band offset. Therefore, Fig. 4 explains the experimentally demonstrated control of the EB. The LSMO EB is determined by the magnetic order of the last layer of BFO, which may be partially pinned by the AF BFO bulk order[25] or by the interface roughness,[4] but this order is strongly affected by an electric field (through changes in V_0). A magnetic field can also influence the EB by reducing the effective value of J_{AFM} and favoring FM order in the last layer of BFO.

IV. DISCUSSION AND CONCLUSIONS

The results reported here are consistent with the interface magnetization and the exchange bias observed experimentally in Refs. 2 and 4. In our picture, the magnetic reconstruction induced at the BFO/LSMO interface is driven by small modifications on the charge density at the interface due to charge transfer between the two materials. Electron energy loss spectroscopy experiments[4] point against a change in the valence state of Fe. This observation can be reconciled with our model if the charge transfer involves the oxygen ions, a scenario that is supported by *ab initio* calculations[26] reporting a strong Fe-O hybridization near the Fermi energy. Our model includes the oxygen electrons implicitly through the double exchange hopping so that the qualitative trends, namely the relation between charge transfer and magnetic reconstruction, remain valid within our approximation.

To conclude, a model that explains the recently unveiled properties of the BFO/LSMO interface is proposed. The charges and spins couple via the DE and superexchange mechanisms, and our calculations show that the induced magnetic moment in BFO arises from charge transfer between the two materials. The spin arrangement generated at the BFO interfacial layer arises from the frustrating effect caused by the two competing (FM and AFM) tendencies in adjacent layers with different electronic densities.[18] Our main result is that changing the sign of the BFO ferroelectric polarization modifies the extra charge near the interface, which in turn strongly affects the magnitude and direction of the magnetic moment. This gives rise to the experimentally observed magnetoelectric coupling, and clarifies the origin of the recently observed electric-field controlled exchange bias in LSMO/BFO heterostructures.

ACKNOWLEDGMENTS

M.J.C. and L.B. acknowledge funding from MICINN (Spain) through Grant No. FIS2009-08744. M.J.C. also acknowledges the Ramón y Cajal program, MICINN (Spain). J.S. acknowledges the European Research Council Starting investigator Award STEMOX 239739. S.L., A.M., and E.D. are supported by the US Department of Energy, Office of Basic Energy Sciences, Materials Sciences and Engineering Division.

[1] W. Eerenstein, N. D. Mathur, and J. F. Scott, Nature (London) **442**, 759 (2006).

[2] S. M. Wu, S. A. Cybart, P. Yu, M. D. Rossell, J. X. Zhang, R. Ramesh, and R. C. Dynes, Nat. Mater. **9**, 756 (2010).

[3] N. A. Spaldin, S.-W. Cheong, and R. Ramesh, Phys. Today **63**(10), 38 (2010).

[4] P. Yu, J.-S. Lee, S. Okamoto, M. D. Rossell, M. Huijben, C.-H. Yang, Q. He, J. X. Zhang, S. Y. Yang, M. J. Lee, Q. M. Ramasse, R. Erni, Y.-H. Chu, D. A. Arena, C.-C. Kao, L. W. Martin, and R. Ramesh, Phys. Rev. Lett. **105**, 027201 (2010).

[5] D. Niebieskikwiat, L. E. Hueso, J. A. Borchers, N. D. Mathur, and M. B. Salamon, Phys. Rev. Lett. **99**, 247207 (2007).

[6] Z. Sefrioui, C. Visani, M. J. Calderón, K. March, C. Carrétéro, M. Walls, A. Rivera-Calzada, C. León, R. López Antón, T. R. Charlton, D. Imhoff, L. Brey, M. Bibes, J. Santamaría, and A. Barthélémy, Adv. Mater. **22**, 5029 (2010).

[7] J. Chakhalian, J. W. Freeland, H.-U. Habermeier, G. Cristiani, G. Khaliullin, M. van Veenendaal, and B. Keimer, Science **318**, 1114 (2007).

[8] J. Garcia-Barriocanal, F. Y. Bruno, A. Rivera-Calzada, Z. Sefrioui, N. M. Nemes, M. Garcia-Hernández, J. Rubio-Zuazo, G. R. Castro, M. Varela, S. J. Pennycook, C. Leon, and J. Santamaria, Adv. Mater. **22**, 627 (2010).

[9] J. Salafranca, M. J. Calderón, and L. Brey, Phys. Rev. B **77**, 014441 (2008).

[10] S. Okamoto, Phys. Rev. B **82**, 024427 (2010).

[11] S. Dong, K. Yamauchi, S. Yunoki, R. Yu, S. Liang, A. Moreo, J.-M. Liu, S. Picozzi, and E. Dagotto, Phys. Rev. Lett. **103**, 127201 (2009).

[12] E. Dagotto, T. Hotta, and A. Moreo, Phys. Rep. **344**, 1 (2001).

[13] C. Israel, M. J. Calderón, and N. D. Mathur, Mat. Today **10**, 24 (2007).

[14] C. Şen, G. Alvarez, and E. Dagotto, Phys. Rev. Lett. **105**, 097203 (2010).

[15] L. Brey, Phys. Rev. Lett. **92**, 127202 (2004).

[16] L. Brey, Phys. Rev. B **75**, 104423 (2007).

[17] S. Dong, R. Yu, S. Yunoki, G. Alvarez, J.-M. Liu, and E. Dagotto, Phys. Rev. B **78**, 201102(R) (2008).

[18] R. Yu, S. Yunoki, S. Dong, and E. Dagotto, Phys. Rev. B **80**, 125115 (2009).

[19] C. Lin, S. Okamoto, and A. J. Millis, Phys. Rev. B **73**, 041104 (2006).

[20] H. Yang, H. M. Luo, H. Wang, I. O. Usov, N. A. Suvorova, M. Jain, D. M. Feldmann, P. C. Dowden, R. F. DePaula, and Q. X. Jia, Appl. Phys. Lett. **92**, 102113 (2008).

[21] M. D. Jong, V. A. Dediu, C. Taliani, and W. R. Salaneck, J. Appl. Phys. **94**, 7292 (2003).

[22] V. Ferrari, M. Towler, and P. B. Littlewood, Phys. Rev. Lett. **91**, 227202 (2003).

[23] A. Nucara, A. Perucchi, P. Calvani, T. Aselage, and D. Emin, Phys. Rev. B **68**, 174432 (2003), and references therein.

[24] C. Broyden, Math. Comp. **19**, 577 (1965).

[25] H. Ohldag, A. Scholl, F. Nolting, E. Arenholz, S. Maat, A. T. Young, M. Carey, and J. Stóhr, Phys. Rev. Lett. **91**, 017203 (2003).

[26] S. J. Clark and J. Robertson, Appl. Phys. Lett. **90**, 132903 (2007).